Manuscript for submission to Boundary-Layer Meteorology

The influence of thermal effects on the wind speed profile of the coastal marine boundary layer

by

Bernhard Lange
University of Oldenburg, Oldenburg, Germany

Søren Larsen,
Jørgen Højstrup
Rebecca Barthelmie
Risø National Laboratory, Roskilde, Denmark

Corresponding author address:

Bernhard Lange
University of Oldenburg
Faculty of Physics
Department of Energy and Semiconductor Research
D-26111 Oldenburg
Germany
Phone: +49-441-798 3927
Fax: +49-441-798 3326
e-mail: Bernhard.Lange@uni-oldenburg.de

Abstract

The wind speed profile in a coastal marine environment is investigated with data from the measurement program Rødsand, where meteorological data are collected with a 50 m high mast in the Danish Baltic Sea, about 11 km from the coast. When compared with the standard Monin-Obukhov theory the measured wind speed increase between 10 m and 50 m height is found to be systematically larger than predicted for stable and partly for near-neutral conditions. The data indicate that the deviation is smaller for short (10-20 km) distances to the coast than for larger (>30 km) distances.

The theory of the planetary boundary layer with an inversion lid offers a qualitative explanation for these findings: When warm air is advected over colder water, a capping inversion might develop. The air below is constantly cooled by the water and gradually develops into a well-mixed layer with near-neutral stratification. Typical examples as well as scatter plots of the data are consistent with this explanation. The deviation of measured and predicted wind speed profiles is shown to be correlated with the estimated height and strength of the inversion layer.

Key Words: Atmospheric Stratification; Coastal influences; Marine boundary layer; Monin-Obukhov theory; Wind speed profile

1 Introduction

Monin-Obukhov theory, although developed from measurements over land, has been found to be generally applicable over the open sea (see e.g. Edson and Fairall (1998)). In homogenous and stationary flow conditions, it predicts a log-linear vertical profile of the wind speed in the atmospheric surface layer:

$$u(z) = \frac{u_*}{\kappa}\left[\ln\left(\frac{z}{z_0}\right) - \Psi_m\left(\frac{z}{L}\right)\right] \quad (1)$$

The wind speed u at height z is determined by friction velocity u_*, aerodynamic roughness length z_0 and Obukhov length L. κ denotes the von Karman constant, taken as 0.4, and Ψ_m is an universal stability function. Thus, if the wind speed is known at one height, the friction velocity can be derived from eq. 1 and the vertical wind speed profile is determined by two parameters: the surface roughness z_0 and the Obukhov length L.

In coastal waters, when wind is blowing from land over the sea, the coastline constitutes a pronounced change in roughness and heat transfer. It poses a strong inhomogeneity to the flow, which may limit the applicability of Monin-Obukhov theory. Stimulated by measurements of large wind stress over Lake Ontario, Csanady (1974) described the processes governing the flow regime under the condition of warm air advection over colder water. He developed a theory of a well-mixed layer with a capping inversion for this condition. His theory is for equilibrium conditions only, and therefore does not describe the development of the flow regime in space and time. From measurements in the Swedish Baltic Sea, Smedman et al. (1997) develop a theoretical explanation of the flow regime over coastal waters under conditions of warm air advection, which also describes the evolution of the mixed layer. They use the travel time of the air over the water surface as additional parameter.

In this study we use data from the meteorological monitoring program at Rødsand in the Danish Baltic Sea to investigate the applicability of Monin-Obukhov theory to predict the wind speed profile at this site. Aim of this paper is to show that:

1. the vertical wind speed profile over coastal waters can deviate substantially from Monin-Obukhov prediction
2. this deviation is systematic for frequently occurring conditions and thus will have an effect on the wind climatology
3. the flow regime leading to this deviation can qualitatively be understood with the theory by Csanady (1974)

The structure of the paper is as follows: In the next section the measurements and data analysis are presented. Section 3 compares the measured wind speed increase with height with Monin-Obukhov prediction and investigates different ways to derive the necessary parameters L and z_0. A qualitative explanation for the deviations found there is offered in section 4. Conclusions are drawn in the last section.

2 The Rødsand field measurement program

2.1 Site

A 50 m high meteorological measurement mast has been established at Rødsand in October 1996 as part of a Danish study of wind conditions for proposed offshore wind farms. The mast is situated about 11 km south of the island Lolland in Denmark (11.74596°E, 54.54075°N) (see Figure 1). It is located in 7.7 m mean water depth with an upstream fetch (distance to coast) of 30 to more than 100 km for wind directions from SE to WNW (120°N to 290°N). In the NW to N sector (300°N to 350°N) the fetch is 10 to 20 km. The present study uses data from March 1998 to January 2000, when wave and current measurements were performed simultaneously to the meteorological measurements.

2.2 Instrumentation and Measurements

The measurement mast is a 48 m high triangular lattice tower with a tower side length of about 1.3 m at the bottom (about 2 m above mean sea level) and about 1 m at 20 m height. Instruments are mounted on booms with boom lengths of about 2.5 m. The instrumentation of the measurement mast is listed in Table 1. About 8500 half-hourly records with simultaneous wind and wave measurements have been recorded. A detailed description of the instrumentation and data can be found in Lange et al. (2001).

Cup anemometers and wind vane

Mean wind speeds and variances are derived from cup anemometers located at three heights (see Table 1). Calibrated instruments of the type Risø P2546a are used. The distance constant Λ of the anemometers is about 2 m. For the measurement heights of 10 to 50 m, which have been used at Rødsand, the ratio z/Λ is in the range of 5 to 25. For such large ratios z/Λ the overspeeding effect can be assumed to be small and the dominant bias is due to variation of the lateral velocity (v-bias), which decreases only slightly with height (Kristensen, 1998). The calibration accuracy is estimated to be +/- 1%. Data are corrected for flow distortion errors due to the mast and the booms with a method developed by Højstrup (1999). Records from situations of direct mast shade have been omitted. The overall uncertainty of the wind speed measurement with cup anemometers is estimated to be +/- 2% and additionally +/- 0.1 ms^{-1}.

A wind vane of the type Risø Aa 3590 is used. The uncertainty of the instrument itself is negligible, but adjustment of the orientation of the instrument is difficult in the field and the absolute accuracy is estimated to be about +/-5º.

Sonic anemometer

The sonic anemometer is of the type Gill F2360a and is mounted at 46.6 m height (at 42.3 m height from 12 May 1999) above mean sea level. It measures wind speed in three components (x,y,z) and air temperature with a resolution of 20 Hz.

Co-variances are calculated from the sonic anemometer measurements with linear trends removed before the calculation. Friction velocity is calculated with the eddy-correlation method as:

$$u_* = \left(\overline{u'w'}^2 + \overline{v'w'}^2 \right)^{0.25} \quad (2)$$

The mean wind speed has been corrected for flow distortion due to mast and booms. Additionally, sonic anemometers experience an array flow distortion, since transducers and struts of the instrument distort the wind flow in the measurement volume. For the horizontal wind speed component flow distortions are corrected with a sensor specific calibration. This is not the case for the vertical wind component. The estimated accuracy is about +/-5% for the horizontal wind speed component and +/-10% for the friction velocity.

Additionally, a statistical uncertainty due to the sampling variability has to be considered. Using the approximation of Wyngaard (1973) derived from the Kansas data, the expected accuracy for the u_* measurements is about 10% for an eddy-correlation measurement at 45 m height with an averaging time of 30 minutes and a mean wind speed of 10 ms^{-1}.

Temperature sensors

For the air temperature measurement at 10 m height a PT100 sensor with radiation shield was used. The water temperature was measured with a PT100 sensor about 2 m below mean sea level. For the temperature difference measurement two PT500

sensors with radiation shields were employed. No mechanical ventilation was used for the radiation shields.

Wave and current measurement

Waves are measured by an acoustic wave recorder (AWR), which is a SONAR-type instrument positioned under water. The type is the HD-AWR201 from DHI Water and Environment, Denmark. Wave height and water depth are derived from the time series of water elevation measured by the AWR. The phase speed at peak frequency c_p is calculated using the measured water depth and the spectral peak frequency f_p, which is determined from the measured wave spectra. The derivation of the wave parameters from the measurements is discussed in detail in Lange et al. (2003).

The water current sensor is a two dimensional electromagnetic sensor measuring the horizontal water velocity, manufactured by GMI (Geophysical and Marine Instrumentation, Denmark). It is located 5.3 m above the sea bottom. The measurement accuracy of the sensor is estimated to be +/- 2%.

2.3 Data processing

Correction of the sonic anemometer measurements for elevation

As a first approximation it is usually assumed that the fluxes in the surface layer are independent of height, implying that the friction velocity and heat flux are constant. However, this assumption is not entirely correct and simple correction procedures have been applied to account for the small decrease of the fluxes with height.

Panofsky (1973) derives the following simplified expression for the height correction of the friction velocity for near neutral conditions from an analysis of the horizontal momentum equation at the surface and the top of the boundary layer:

$$u_*(z) = u_{*s} - 6 f_c z \qquad (3)$$

Here $u_*(z)$ is the friction velocity measured at height z, u_{*s} is the friction velocity at the surface and f_c the Coriolis parameter ($1.46\ 10^{-4}\ \sin(\phi)$, with ϕ latitude). This leads to a correction of 0.03 ms^{-1}, which has been used as a first order correction for all records.

Lenschow et al. (1988) give an empirical relation for the decrease of the covariance of vertical wind speed and temperature, $\overline{w'T'}$, from its surface value $\overline{w'T'}_s$:

$$\overline{w'T'}_s = \begin{cases} \overline{w'T'}(z)\dfrac{1}{\left(1-\dfrac{z}{z_i}\right)^{1.5}} & \textit{for stable conditions} \\ \overline{w'T'}(z)\dfrac{1}{1-1.5\dfrac{z}{z_i}} & \textit{for unstable conditions} \end{cases} \qquad (4)$$

where $z_i=0.25u_*/f_c$ is used to estimate the boundary layer height (Tennekes, 1982). This is only valid for near-neutral conditions, but is used here as a first order correction for all cases.

Transformation of wind speeds to water following co-ordinates

For a flow over a moving surface the relevant flow speed is the difference between flow and surface movement. When water currents are present, wind measurements made from fixed structures, like the measurement mast at Rødsand, therefore need to be transformed to the reference frame of the sea surface. At Rødsand, the water current is measured at a mean water depth of 2.4 m. Differences between the current at this depth and the surface current have been neglected and all mean wind speeds measured at the mast have been transformed to refer to the moving reference frame of the water surface. At Rødsand currents are generally weak, usually below 0.4 ms^{-1},

and differences in wind speed due to the transformation are therefore small (less than 3% wind speed difference for 95% of the records).

Data selection

Situations with fast temporal changes in flow conditions are not correctly described by Monin-Obukhov theory. Records with fast changes in atmospheric conditions have therefore been omitted for the analysis. For the important quantities the record under investigation was compared to the two previous and the following record and records with large changes were rejected (54% of the data). This was done for wind speed, wind direction and temperature measurements and for the derived stability parameters (see section 3.1.1). Differences of less than 20% were required for wind speed, 15º for wind direction, 0.5ºC for air temperature and 0.2ºC for water temperature. A maximum change of atmospheric stability of 10/L=0.1 has been applied, where L is the Obukhov length determined from the three methods described in section 3.1.1.

For low wind speed cases the top of the atmospheric surface layer might be lower than the measurements at 50 m and 45 m height. Using again the simple approximation for the height of the boundary layer, $z_i=0.25u_*/f_c$, and assuming that the height of the surface layer is about 10% of this, leads to a limiting value for u_* of about 0.2 ms^{-1}. Measurements with smaller u_* have been rejected (41% of the data). 1892 half-hourly records are used in the final database.

2.4 Air temperature measurements over land

The wind speed, wind direction and air temperature over land in the upwind direction from Rødsand have been estimated from measurements at synoptic stations of the German Weather Service (DWD) and the measurement station Tystofte in Denmark (operated by the Risø National Laboratory). Seven stations on mainland Germany

close to the coast were selected, which cover wind blowing towards Rødsand from west, south and east (see Figure 1). The measurement station Tystofte is about 80 km north of Rødsand, but is assumed to give a fair approximation of the air temperature over land for a wind direction sector from 300º to 030º. Measurement height at all land stations is 2 m for air temperature and 10 m for wind speed and direction. The direction of the geostrophic wind has been determined from the Rødsand measurement with the geostrophic drag law (Garratt,1994). From the German stations the measured temperatures of those stations with upwind direction closest to this geostrophic wind direction have been linearly interpolated to estimate the upwind air temperature over land for Rødsand. For wind speed and direction the measurements of the closest upwind station have been used.

3 Prediction of wind speed profiles with Monin-Obukhov theory

3.1 Influence of stability on the vertical wind speed profile

3.1.1 Derivation of the Obukhov length

Atmospheric stability is described in Monin-Obukhov theory with the Obukhov length scale L as stability parameter. Three different ways to derive this parameter are considered:

1. L has been derived directly from the sonic anemometer measurements of u_* and $\overline{w'T'}$ (Sonic method).

2. It has been derived via the Richardson number from the temperature and wind speed difference measurements at 10 m and 50 m (Gradient method).

3. It is estimated from the air and water temperature measurements and one wind speed measurement at 10 m height (Bulk method).

No humidity measurement is available at Rødsand. Therefore only an average humidity flux could be accounted for in the calculation of the stability parameters. Following Geernaert and Larsen (1993), a relative humidity of 100% and 70% has been assumed at the surface and at 10 m height, respectively. The measured water temperature has been used to transform these to absolute humidity. The humidity scale q_* and the vertical humidity profile have been calculated with a diabatic profile with standard humidity stability functions and a humidity roughness length of $z_{0q}=2.1\cdot10^{-4}$ m (see Geernaert and Larsen (1993)).

Sonic method

L is determined directly from sonic anemometer measurements of friction velocity and heat flux by:

$$L_{sonic} = -\frac{u_{*,s}^{\ 3}}{\kappa \frac{g}{\overline{T}} \overline{w'T'}_s} \qquad (5)$$

Here $\overline{w'T'}_s$ is the covariance of temperature and vertical wind speed fluctuations at the surface, u_{*s} the surface friction velocity, $\overline{T}$ the reference temperature, g the gravitational acceleration and κ the von Karman constant (taken as κ=0.4).

The sonic anemometer measures sound virtual temperatures, which differ from virtual temperatures by $0.1\overline{T}\ \overline{w'q'}$ (Schotanus et al., 1983):

$$\overline{w'T'_{sonic}} = \overline{w'T'} + 0.51\overline{T}\ \overline{w'q'} = \overline{w'\Theta'_v} - 0.1\overline{T}\ \overline{w'q'} = \overline{w'\Theta'_v} - 0.1\overline{T}u_*q_* \qquad (6)$$

Here q is the absolute humidity and Θ_v the virtual potential temperature. The assumptions for the humidity stated above have been used for the estimation of q_*.

Gradient method

Temperature and wind speed difference measurements at 10 m and 50 m height are used to estimate the gradient Richardson number Ri_Δ:

$$Ri_\Delta(z') = \frac{\frac{g}{\overline{T}}\left(\frac{\Delta\overline{T_v}}{\Delta z} + \frac{g}{C_p}\right)}{\left(\frac{\Delta\overline{u}}{\Delta z}\right)^2} \tag{7}$$

Here $\Delta T/\Delta z$ is the virtual temperature difference ΔT_v at a vertical height difference Δz. Equally, $\Delta u/\Delta z$ is the wind speed difference Δu at the vertical height difference Δz. C_p is the specific heat of air at constant pressure. Humidity at the two heights has been estimated as described above. The height z' at which this Ri number is valid can be estimated as $z' = (z_1 - z_2)/\ln(z_1/z_2)$ (Larsen, 1993). Assuming the applicability of Monin-Obukhov theory, the gradient Richardson number is converted to L by means of the following relation based on the Kansas results (Businger et al., 1971, Högström, 1988):

$$L_{Gradient} = \begin{cases} \left(\frac{z'}{Ri}\right) & Ri < 0 \\ \frac{z'(1-5Ri)}{Ri} & 0 < Ri < 0.2 \end{cases} \tag{8}$$

Bulk method

Air and sea temperature measurements together with the wind speed at 10 m height are used with an approximation method proposed by (Grachev and Fairall, 1997).

Humidity has been accounted for by calculating the virtual temperatures with the assumptions stated above.

For the bulk method the sea surface temperature is required. This is not measured at Rødsand and therefore had to be replaced by the water temperature measured at a depth of about 2 m. Due to the cool skin effect this temperature is on average slightly higher than the skin temperature (Fairall et al., 1996). This leads to a small but systematic overprediction of the temperature difference between the surface and 10 m height and consequently to an overprediction of the stability parameter |10/L|, i.e. the calculated values of 10/L are too high for stable and too low for unstable conditions.

3.1.2 Comparison of predicted and measured wind speed profile

The wind speed ratio between 50 m and 10 m height is predicted using Monin-Obukhov theory. From the diabatic wind profile (see eq. 1) the wind speed ratio is calculated as:

$$\frac{u(z_2)}{u(z_1)} = \frac{\left[\ln\left(\frac{z_2}{z_0}\right) - \Psi_m\left(\frac{z_2}{L}\right)\right]}{\left[\ln\left(\frac{z_1}{z_0}\right) - \Psi_m\left(\frac{z_1}{L}\right)\right]} \qquad (9)$$

Here z_0 is the aerodynamic roughness length and $\Psi_m(z/L)$ the integrated stability function, for which the Businger-Dyer formulation (Businger et al., 1971) is used. For the empirical parameters β and γ the values of the Kansas measurement reanalysed by Högström (1988) for a von Karman constant of 0.4 are used (β=4.8 and γ=19.3).

$$\Psi_m = \begin{cases} 2\ln\left(\frac{1+\Phi_m{}^2}{2}\right) - 2\tan^{-1}(\Phi_m) + \frac{\pi}{2} & with\ \Phi_m = \left(1-\gamma\frac{z}{L}\right)^{1/4} \quad for\ z/L < 0 \\ -\beta\frac{z}{L} & for\ z/L > 0 \end{cases} \tag{10}$$

The aerodynamic roughness length of the sea is estimated with the Charnock relation (Charnock, 1955):

$$z_0 = z_{ch}\frac{u_*^2}{g} \tag{11}$$

The Charnock parameter is taken as z_{ch}=0.0185 (Wu, 1980). The influence of different methods to estimate the sea surface roughness on the prediction of the vertical wind speed profile will be investigated and compared in section 3.2.

The theoretical dependency of the wind speed ratio u(50)/u(10) on the stability parameter 10/L is compared with the Rødsand measurements in Figure 2 to Figure 4, where the measured ratios are plotted versus the three different Obukhov lengths derived from the measurements as described in the previous section.

In Figure 2 the sonic method is used to determine L. The measured wind speed ratios show large scatter when plotted versus L derived by the sonic method. This can at least partly be explained by the sampling variability of the friction velocity measurement (see section 2.2), which has a large impact on L since it is cubed in the calculation (see eq. 5). In comparison with the prediction of Monin-Obukhov theory the agreement is best for unstable conditions (10/L<-0.05). For near-neutral and stable situations systematic deviations are found. The wind speed ratio is generally higher than expected. This is especially obvious for conditions, which are close to neutral on the stable side. Here the measured ratios are systematically higher than expected from

theory. Data with northerly wind directions (295º-075º), where the distance to the coast (fetch) is smallest, are marked with grey squares in the figure. These data show a different behaviour and seem to agree better with the theory for stable conditions, though with a very large scatter.

The result for L derived with the gradient method is shown in Figure 3. The data show less scatter compared to the sonic method since no co-variances are used in the determination of L. Again a good agreement is found in the unstable region, while for stable conditions the deviations are even more pronounced. The wind speed ratio is systematically higher than predicted by Monin-Obukhov theory and the deviation increases with increasing stability parameter 10/L. The data from short fetches show again smaller ratios, which are, however, still higher than the theoretical prediction. The deviation from Monin-Obukhov prediction is larger than for the sonic method, which can be understood from the way in which L is calculated. In the determination of L with the gradient method the applicability of Monin-Obukhov theory has been assumed (eq. 8). This means that the wind speed ratio between 10 m and 50 m height, which is predicted, is already included in the calculation of L. From eq. 7, 8 and 10 it can be seen that the diabatic term in the vertical wind profile is inversely proportional to the wind speed height ratio squared ($\Psi_m(z/L) \sim 1/\Delta u^2$) for stable stratification. Therefore any deviation between measured and predicted profile is amplified with this method.

For the bulk method the measured ratios versus 10/L are shown in Figure 4. Here again the scatter is smaller than for the sonic method. As for the other two methods, the agreement is good for unstable data and systematically higher ratios are found for stable conditions compared with theory. The deviations are smallest for the bulk method. Short fetch data show again on average smaller ratios and for the bulk

method and a systematic deviation of these data from theoretical predictions can not be seen. The small magnitude of the deviation in the bulk method is due to the fact that only an absolute wind speed and not a wind speed difference enters in the calculation of L. In contrary to the gradient method a deviation of the measured from the predicted profile will therefore only lead to a small relative difference in the calculation of L. Additionally, the systematic error caused by using the bulk water temperature instead of the sea surface temperature (see section 3.1.1) leads to an overprediction of 10/L on the stable side. This partly compensates the deviations between measured and predicted wind speed profile.

The ratio between measured and predicted wind speed at 50 m height, $u50_{meas}/u50_{pred}$, has been built, where the prediction is made from the measured wind speed at 10 m height with eq. 9:

$$\frac{u(50)_{meas}}{u(50)_{pred}} = \frac{u(50)}{u(10)} \frac{\left[\ln\left(\frac{10}{z_0}\right) - \Psi_m\left(\frac{10}{L}\right)\right]}{\left[\ln\left(\frac{50}{z_0}\right) - \Psi_m\left(\frac{50}{L}\right)\right]} \qquad (12)$$

The deviation of this ratio from 1 gives a measure of the deviation of the measured profile from Monin-Obukhov theory. The bin-averaged ratios $u50_{meas}/u50_{pred}$ for the three different methods to derive L are compared in Figure 5 together with their standard errors. Only bins with more than 20 records are shown. It can be seen that the deviations between measurement and Monin-Obukhov theory increase with increasing stability parameter 10/L for all methods to derive L, with the exception of the sonic method for stable conditions. Deviations are between 0% and 3% for unstable conditions and between 3% and 17% for stable conditions.

3.2 Influence of roughness on the vertical wind speed profile

3.2.1 Models to estimate the sea surface roughness

Compared to land surfaces the surface roughness of water is very low. Additionally, it is not constant, but depends on the wave field, which in turn is determined by the wind speed, distance to coast (fetch), etc. It is investigated how different models to describe the sea surface roughness influence the prediction of the wind profile (eq. 1) and thus might explain the deviations of the measured wind profile from the predictions of Monin-Obukhov theory. Three models for the sea surface roughness z_0 are considered:

1. A constant z_0 is assumed.

2. The classical Charnock approach relating sea surface roughness to friction velocity is used.

3. An extension of the Charnock relation is considered, which takes into account the influence of fetch on the sea surface roughness by means of the wave age.

Constant roughness

The assumption of a constant sea surface roughness is often used in applications because of its simplicity, e.g. in the wind resource estimation program WAsP (Mortensen, 1993). A value of z_0=0.2 mm is assumed.

Charnock relation

The most common model taking into account the wave field by its dependence on friction velocity is the Charnock relation (Charnock, 1955) (see eq. 11). The

Charnock parameter z_{ch} is assumed to be a constant. The standard value of z_{ch}=0.0185 has been used (Wu, 1980).

For comparison, the Charnock parameter has also been determined from the measurement data. Because of the deviations found above only unstable data ($10/L_{sonic}$<-0.05) were used. A Charnock parameter of 0.03 was found, which is higher than the standard value, but still in the range of other experimental values found for limited fetch conditions (see Garratt, 1994).

Wave age dependent model

The Charnock relation works well for the open ocean, but for coastal areas it was found that the Charnock parameter is site specific, due to the influence of other physical variables like fetch on the wave field. An extension of the Charnock relation by a parameterisation of the Charnock parameter with wave age as additional parameter by Johnson et al. (1998) is used:

$$z_{ch} = A\left(\frac{c_p}{u_*}\right)^B \qquad (13)$$

Here c_p/u_* is the wave age, the ratio of the velocity of the peak wave component c_p and the friction velocity u_*. The values for the empirical constants A and B are taken from Johnson et al. (1998) as A=1.89 and B=-1.59. A comparison of this model with the Rødsand data can be found in Lange et al. (2003).

3.2.2 Comparison of predicted and measured wind speed gradients

The three sea surface roughness models have been used to predict the wind speed at 50 m height from the 10m wind speed. The ratios $u50_{meas}/u50_{pred}$ are shown in Figure

6 for the bulk method as example. The difference of the results with the different z_0 models is much smaller than the difference between the different methods to derive L. They can therefore not be the reason for the deviations found. For near-neutral conditions the wave age model yields slightly smaller and the constant z_0 slightly larger deviations compared to the Charnock model.

3.3 Average deviations

The extrapolation of the wind speed from 10m to 50m has been tested. The ratio between measured and estimated 50 m wind speed has been built with all models and its bias and rms-error calculated. It is given in the left two columns of Table 2. From the models to derive L the bias and rms-error are lowest for the bulk method. For the sea surface roughness the constant value, shows the smallest deviation both with respect to bias and rms-error.

The data were also divided into cases with stable and unstable atmospheric conditions (see Table 2). The Obukhov-length L used for the selection was determined with the sonic method. It can be seen that the bias is very different between both conditions. The rms-errors are about the same when L is determined with the sonic method, but different for the other two methods. The comparison shows clearly the large deviations from theory in the stable regime.

4 The inhomogeneous flow regime in the coastal zone

4.1 Qualitative description of the flow regime

The measurement station Rødsand is surrounded by land in distances between 10 and 100 km and thus the air in the boundary layer will always be advected from land. Due

to the large differences in heat capacity and conduction between land and water the air over land will often be warmer than the sea surface temperature. Especially at daytime, when the land is heated by the sun, and in early spring, when the water temperature is still low from winter, warm air is advected over the colder sea to the measurement station. Large temperature differences between the advected air and the sea surface can occur. At Rødsand temperature differences of up to 9ºC were measured.

The flow regime which develops in this situation has been described by several authors (see e.g. Csanady (1974), Garratt (1987), Garratt and Ryan (1989), Melas (1989), Tjernström and Smedman (1993), Smedman et al. (1997)). We follow the explanation given by Csanady (1974) and Smedman et al. (1997): When warm air is blown over the cold sea, an internal boundary layer will develop at the shoreline due to the roughness and heat flux change. In the case of warm air advection over cold sea this is a stable internal boundary layer (SIBL), since the air close to the sea surface will be cooled. The SIBL is characterised by low turbulence and therefore small fluxes and slow growth. The warm air is cooled from below while the sea surface temperature will remain almost constant in this process due to the large heat capacity of water. Eventually, the air close to the sea surface will have the same temperature as the water and the atmospheric stability will be close to neutral at low heights. Above the internal boundary layer the air still has the temperature of the air over land and near the top of the SIBL an inversion lid has developed with strongly stable stratification separating these two regions. Thus, while the stability in the mixed layer is close to neutral, the elevated stable layer influences the wind speed profile and leads to a larger wind speed gradient than expected for an ordinary near neutral condition.

Due to the small fluxes through the inversion lid this flow regime is a quasi-equilibrium state and can survive for large distances before eventually the heat flow through the inversion evens out the difference in potential temperatures. Eventually the neutral boundary layer is recovered, which is known from open ocean observations (Edson and Fairall, 1998).

4.2 Qualitative comparison with Rødsand data

Two example cases have been selected, where large deviations of the measured and predicted wind speed ratio at 10 and 50 m height prevailed for a longer time period. Their time series are plotted in Figure 7 and Figure 8.

Figure 7 shows a time series of 48 hours, 15 and 16 January 1999. In the uppermost graph, air and water temperatures at Rødsand are shown along with the air temperature over the upwind land. Temperature differences between air over land and water range from about 1 to 7ºC and a situation of warm air advection over colder sea is present for the whole time period. The air temperature measured at Rødsand is very close to the land air temperature at the beginning of the period, but from 1200 at the first day a difference between air temperatures over land and at Rødsand can be seen, most pronounced at the afternoons of both days, where a temperature difference of about 3ºC is reached (see vertical lines in Figure 7).

The wind direction (see second graph) at Rødsand varies between 200º and 270º until 1800 on the first day and stays almost constant at about 200º from than until almost the end of the time period. The wind direction over land, upwind from Rødsand, shows mainly lower values up to the afternoon of the first day and higher or equal values afterwards.

Wind speed at 10 m height (see second graph) at Rødsand is more variable during the first period with values between 8 and 14 ms^{-1}. On the second day it slowly increases from 8 to 13 ms^{-1} and slightly decreases at the end of the measurement period to about 11 ms^{-1}. The wind speed over land, upwind from Rødsand, is lower, especially during the nights.

The third graph shows the ratio $u50_{meas}/u50_{pred}$ between measured and predicted 50 m wind speed, where the three different methods to derive L have been used: sonic, gradient and bulk. The Charnock relation has been used for the sea surface roughness. Large deviations between measured and predicted 50 m wind speed can be seen, up to about 20% for the gradient, 15% for the sonic and 10% for the bulk method. The variation of these deviations shows a correlation with the air temperature over land when the bulk or gradient methods are used for the prediction. It can be seen that the deviations are largest in the afternoon of both days (see lines). When the sonic measurement is used to derive L and predict the 50 m wind speed the scatter in the ratio $u50_{meas}/u50_{pred}$ is larger and a pattern following the air temperature over land can not be seen. The lowest graph will be discussed in section 4.3.

Figure 8 shows a time series of one day (24 January 1999), where the temperature difference between air over land and sea varies between 2 and 5ºC, i.e. again a situation of warm air advection over colder sea. The air temperature over sea is only slightly lower (0-1ºC) than over land most of the time. Only in the afternoon a larger temperature difference of up to 3°C is found (see vertical line in Figure 8). Wind direction at Rødsand varies between 200º and 250º at wind speeds of 7-11ms^{-1}. Wind direction values over land are close to or below those at Rødsand most of the time. However, as in the first example, in the afternoon the unusual turn in wind direction to the left for wind blowing from land to sea can be seen again (see line). Ratios

$u50_{meas}/u50_{pred}$ are similar to those in the first example with higher deviations starting in the afternoon (see line), where also the air temperature over land is highest.

The conceptual model discussed in section 4.1 can explain the effects found in the two examples: In the first time series (Figure 7), air temperatures over land and at Rødsand are almost equal at the beginning of the first day, while the sea temperature is slightly (1-2°C) lower. Between 1200 and 1800 that day the air temperature over land rises significantly (about 3°C), while the air temperature over sea remains almost constant. In the second time series (Figure 8) a similar behaviour can be seen around 1400, where the air temperature over land is more than 2°C warmer than over sea. The difference in air temperatures between land and sea indicates that a difference in potential temperature has developed at Rødsand between the air at greater height, which is advected from land and therefore has the potential temperature of the land temperature, and the air at 10 m height, which has been cooled from the sea. The large difference at the afternoons (see vertical lines) indicate that an elevated stable inversion layer with a large temperature gradient has developed, which is responsible for a large part of this difference. The wind direction differences between land and sea station support this. The wind direction usually turns to the right when blowing from land over sea, due to the lower roughness of the sea surface (see section 4.3). It can be seen here that this turning is compensated or even reverted due to the decoupling of the lower layer from the air above the inversion in the time periods where the elevated inversion layer prevails. This is especially pronounced in the afternoons (see lines). At these time periods also the deviations of the predicted vertical wind speed profile from Monin-Obukhov theory ($u50_{meas}/u50_{pred}$), which are caused by the inversion layer, are large.

To test if this behaviour of the example time series is typical, the deviation of measured and predicted wind speed at 50 m height is plotted versus the difference between air temperature over land and sea temperature for all data. The result is shown in Figure 9, with the gradient method used to determine L and the Charnock relation for z_0 as an example. It can be generalised that for the vast majority of the data with large deviations of $u50_{meas}/u50_{pred}$ from 1 the air temperature measured over land is larger than the sea temperature.

4.3 Comparison of the Rødsand data with theoretical approaches

Csanady (1974) developed a theory for a mixed layer flow with capping inversion. He proposes the so-called buoyancy parameter Bu to predict if such a flow regime will develop:

$$Bu = \frac{b}{fv_g} = g\frac{\Delta\rho}{\rho}\frac{1}{fv_g} \qquad (14)$$

Here g is the gravitational acceleration, b is the buoyant acceleration ($b=g\Delta\rho/\rho$), ρ the air density, $\Delta\rho$ the air density difference between surface and geostrophic level at constant pressure, f the Coriolis parameter and v_g the geostrophic wind speed.

Since only mast data up to 50 m height are available at Rødsand, the geostrophic wind speed and the air density at geostrophic level have to be estimated. The geostrophic wind speed is estimated from the geostrophic drag law (see e.g. Garratt (1994)), with z_0 estimated with the Charnock relation (see section 3.2.1). For the calculation of the air density difference it is assumed that the air at this height is advected from land without temperature change. This is consistent with Csanady's model since the capping inversion only allows a very small heat flux. The potential temperature at geostrophic level is then equal to the potential temperature over land. It is additionally

assumed that the temperature stratification over land is neutral. Then the potential temperature measured over land at 2 m height can be used as an estimation of the potential temperature over sea at geostrophic height.

Csanady (1974) found that an inversion lid is likely to develop if Bu>30. The deviation of measured and predicted 50 m wind speed is shown versus the buoyancy parameter Bu in Figure 10. The gradient method has been chosen here to determine L since it shows the largest deviations. The roughness z_0 is estimated with the Charnock relation. The scaling with Bu leads to a clearly reduced scatter when compared to Figure 9, where only the temperature difference between land and sea is used. Three regions can be distinguished in Figure 10: For negative Bu, i.e. cold air over warmer water, generally small deviations are found. For Bu larger than 30, i.e. warm air over cold water, where an inversion lid should exist, large deviations are found that increase with growing Bu. For intermediate Bu between 0 and 30, i.e. warm air over cold water, but according to Csanady (1974) without inversion lid, a wide range of deviations is found: Two clusters can be distinguished, one with deviations similar to those of negative Bu and one with deviations of an extension of the trend line of large and increasing Bu>30. In the intermediate region both regimes seem to overlap. Data with short fetch (marked with grey squares) show a tendency of smaller deviations. However, these might be outside the applicability of this equilibrium theory. Some conflicting observations occur, probably because the assumption of a neutral stratification over land will inevitably be wrong in some cases. Smedman et al. (1997) argue that not only the temperature difference, but also the travel time of the warmer air above the cold water will determine the development of a mixed layer. They propose a bulk stability parameter S to distinguish between an ordinary stable layer and a mixed layer with capping inversion:

$$S = \sqrt{tf}\,\frac{\Theta}{\Delta\Theta} \tag{15}$$

where $t=X/v_g$ is the travel time (with X=distance to upwind coast and v_g=geostrophic wind speed), f Coriolis parameter, Θ reference temperature, $\Delta\Theta$ temperature difference between air over land and sea. They find that for ordinary stable profiles S<75, while for profiles with near neural stratification and inversion lid S>75.

The Smedman et al. (1997) formulation can be interpreted as an extension of Csanady's theory to conditions with limited fetch. The bulk stability parameter S is connected to Csanady's buoyancy parameter Bu by:

$$S = \frac{g}{\sqrt{f}}\,\frac{\sqrt{X}}{\sqrt{v_g^{\,3}}}\,\frac{1}{Bu} \tag{16}$$

This shows that S and Bu are inversely proportional and have a very different dependency on wind speed.

The deviation of measured and predicted 50 m wind speed is shown versus the bulk stability parameter S in Figure 13. For negative S, i.e. warm air over cold water, deviations are usually small. For positive S, large deviations can be seen, which decrease with increasing S.

For a theory including the development of the flow with increasing fetch, it could be expected that the deviations measured for different fetches collapse when plotted versus S. This is not the case. The data with short fetch show clearly smaller deviations than the data with longer fetch for the same S.

The buoyancy parameter Bu and the bulk stability parameter S are also shown in the example cases (see Figure 7 and Figure 8). Also here high Bu and low S values can be seen for the time periods with large deviations.

The buoyancy parameter Bu or the bulk stability parameter S aim to determine if a mixed layer with inversion lid can develop in a certain situation. The influence of such a flow regime on the wind speed profile can be expected to depend on the depth of this mixed layer. If the inversion is very high it will probably have little influence on the wind speed profile up to 50 m height, while a low inversion height can be expected to have a large impact. Csanady (1974) proposes the following expression for the depth of the mixed layer h in equilibrium conditions:

$$h = A \frac{1}{g} \frac{\rho}{\Delta\rho} u_*^{\,2} \qquad (17)$$

He estimates the empirical parameter A to 500. Tjernström and Smedman (1993) found a reasonable agreement of the height of the inversion predicted with eq. 17 with that estimated from airborne measurements over the Baltic Sea.

The ratio $u50_{meas}/u50_{pred}$ shown versus the mixed layer depth h in Figure 14 (in logarithmic scale). The gradient method has been used to determine L and the Charnock equation for the estimation of z_0. A clear correlation can be seen with large ratios for low inversion heights of a few 100m, decreasing rapidly with increasing inversion height.

It has to be kept in mind that the estimated inversion height h is for equilibrium conditions only, i.e. when the mixed layer and capping inversion already are developed. Therefore the theory can not be used for small fetches. This limitation might be the reason that the deviations of the measured wind speed profile and the Monin-Obukhov prediction found for small fetches (<20km, grey squares) is smaller than for long fetches (>30 km).

A second way of comparing Csanady's theory with the measurements is by looking at the wind direction change when wind blows from land over the sea. According to

Csanady's theory the surface flow over the sea is a mixed layer flow decoupled from the rest of the boundary layer. Csanady (1974) investigates the limiting case of Bu→A, at which h→0 and v→0, i.e. an inversion layer with vanishing height and wind speed. For this case he predicts the difference in wind direction between geostrophic and surface levels (the ageostrophic angle α) to be 90°, i.e. the wind blows along the pressure gradient. This is a large difference to the ageostrophic angle expected for the wind at the land station (approx. 30°), which leads to a difference in surface wind direction between land and sea $\Delta d=(d_{geo}-\alpha_{land})-(d_{geo}-\alpha_{sea})$ of +60°, assuming the same geostrophic wind direction over land and sea.

This difference in ageostrophic angle α is much larger than predicted by conventional theory of ordinary stable boundary layers. For ordinary stable boundary layers, α can be calculated from (see Garratt, 1994; eq. 3.80 and 3.81):

$$\tan\alpha = \frac{\ln\left(\frac{z_i}{z_0}\right) - A_2(\mu)}{-B_2(\mu)} \tag{18}$$

for the northern hemisphere. Here z_i is the height of the boundary layer, z_0 the surface roughness length and $\mu=z_i/L$ a stability parameter with Obukhov-length L. The empirical functions A_2 and B_2 for slightly stable conditions ($0<\mu<35$) are (Garratt, 1994, eq. 3.89):

$$A_2(\mu) = 1 - 0.38\mu \tag{19}$$

$$B_2(\mu) = 4.5 + 0.3\mu \tag{20}$$

The Rødsand data investigated here are slightly stable with L>50 (10/L<0.2, see Figure 2 to Figure 4). Assuming a boundary layer height of z_i<1000m for these slightly stable data leads to $0<\mu<20$. Figure 11 shows variation of the ageostrophic

angle α for this range of the stability parameter for a typical roughness length of land (0.1 m) and sea (0.0001 m). It can be seen that the difference in the ageostrophic angle $\Delta\alpha=\alpha_{land}-\alpha_{sea}$ is in the range of 4° to 12°, assuming neutral conditions over land. This difference $\Delta\alpha$ leads to a difference in surface wind direction between land and sea $\Delta d=(d_{geo}-\alpha_{land})-(d_{geo}-\alpha_{sea})$ of -4° to -12°, assuming the same geostrophic wind direction.

Figure 12 shows the measured difference in surface wind direction Δd versus the buoyancy parameter Bu. The range of Δd expected from conventional theory is shown as well as a line between the limiting values predicted by Csanady's theory: $\Delta d=60°$ at Bu=500 and conventional theory at Bu=0. It has to be stressed that this line is merely to visualise the trend predicted by Csanady (1974), not to show a relationship, which would depend on more parameters than Bu. Data with low wind speeds ($<6ms^{-1}$) have been omitted to reduce scatter.

The scatter in the data is large as can be expected from wind direction measurements taken 60 to 150 km apart. Also, the maximum values of Bu encountered in the measurement are small compared to the limit of Bu=500. However, a trend of increasing Δd with increasing Bu as predicted by Csanady's theory seems plausible from these data. Especially for data with Bu>100 a systematic deviation of Δd from the range expected from conventional theory can be seen. This is also in agreement with the statement in Csanady (1974) that a significant deviation of the ageostrophic angle from conventional theory can only be expected for Bu>100.

5 Conclusion

Data from the measurement program Rødsand have been used to investigate the wind speed profile in the coastal marine surface layer. The 50 m high meteorological mast is located 11 km from land and experiences fetches from 11 to more than 100 km. The measured wind speed ratio between 10 m and 50 m height is found to be systematically larger than expected with Monin-Obukhov theory for most data in near-neutral and for almost all data in stable conditions. The deviations are more pronounced for large overwater fetch (>30km) than for fetches of 10-20 km, in contrary to the intuitive expectation that the importance of coastal influences decreases for increasing fetch.

Different methods to derive the Obukhov length L and the sea surface roughness from the measurements have been compared. The deviations between measured and predicted wind speed profiles were found for all three methods used to derive L. They all predict a smaller wind speed increase from 10 m to 50 m than measured. The magnitude of the deviation differs for different methods to derive L since the methods are differently sensitive for deviations of the wind speed profile. Different methods to estimate the sea surface roughness have also been tested. They only lead to small differences in the wind profiles and can therefore not be responsible for the deviations found between the measured and predicted wind speed increase from 10 m to 50 m.

A qualitative explanation for the failure of Monin-Obukhov theory for the coastal marine boundary layer in near-neutral and stable conditions is offered by Csanady (1974). He describes the flow regime for warm air advection over a colder sea. If certain conditions are fulfilled, an inversion lid with strongly stable stratification will develop at the top of the internal boundary layer with small turbulent transport. The

heat flow through the inversion will therefore be small, while the air below the inversion is cooled continuously from the sea surface. It will eventually take the temperature of the sea and become a well-mixed layer with near-neutral stratification.

The decoupling of the flow below and above the inversion can lead to pronounced wind direction and wind speed changes. It might also be one possible reason for the low-level jets reported earlier for the Baltic Sea (Källstrand, 1998).

In such a situation of strong height variation of atmospheric stability Monin-Obukhov theory must fail and the wind speed ratio between 10 m and 50 m height predicted for this near-neutral or weakly stable stratification is too small. Additionally, the ageostrophic angle between the wind direction at the top of the boundary layer and near the surface will differ from the prediction of conventional theory.

With wind and temperature data from land stations surrounding the Rødsand site it is shown that the deviations in the wind speed profile and surface wind direction depend on the condition of warm air advection over a colder sea, as required by this theory. It can also be seen that measurements with short fetch (<20 km) show smaller deviations. This might indicate that for these fetches the inversion lid is still under development, which could be expected from the theory.

The conditions under which a flow regime of a mixed layer with capping inversion will occur, have been quantified by Csanady (1974) by the buoyancy parameter Bu for equilibrium conditions, i.e. when the inversion lid has been formed. A clear dependency of the deviation in the wind profile on the parameter Bu is found. The data show largest deviations from Monin-Obukhov theory for Bu>30, which is the limit estimated by Csanady for the formation of an inversion lid. The effect of the

inversion lid on the ageostrophic angle can be seen for Bu>100, as estimated by Csanady.

Smedman et al. (1997) extend the theory by taking into account the development of the flow with fetch. They propose a bulk stability parameter S to predict if an inversion develops. A clear dependency of the deviation on S is found, but the influence of fetch on the deviation measured at Rødsand is not captured and overall Bu seems better to match the data.

The deviation between measured and predicted wind speed profile is expected to be influenced not only by the existence of an inversion lid, but also by its height. Csanady (1974) gives a relation for the inversion height h. The comparison with the measurement data reveals a clear correlation between h and the deviation in the wind speed profile. Largest deviations are found for low estimated inversion heights, while for large inversion heights the deviations are small.

These findings strongly support the view that the deviations found in the measurements from standard Monin-Obukhov theory can be qualitatively explained with the existence of a flow regime consisting of a mixed layer with capping inversion as described by Csanady. We conclude that Monin-Obukhov theory can not be applied to the coastal marine boundary layer under conditions of warm air advection even for fetches larger than 30 km. Further research is needed to find an alternative model describing the fluxes and profiles in the coastal marine boundary layer under these conditions.

Since warm air advection occurs frequently in coastal waters, at least in the Baltic Sea, this effect has an important influence on the average vertical wind speed profile and therefore implications also for the wind climatology at such sites. Wind speeds at

greater heights predicted from lower measurements with Monin-Obukhov theory e.g. will systematically be estimated too low. It is important to note that this effect is largest for quite large distances of several tens of kilometres to the upwind coast and not close to the coast, where one would usually expect influences of the coastal discontinuity to be largest.

Acknowledgements

The Rødsand measurement program was funded by the following: JOULE program of the European Union (JOU2-CT93-0325), Office of naval research (N00014-93-1-0360), Danish Energistyrelsen (UVE J.nr. 51171/96-0040) and ELKRAFT. The technical support team at Risø and Mr Kobbernagel of Sydfalster-El are acknowledged for their contribution to the data collection. The air temperature data from the German synoptic stations were made available by the German Weather Service (DWD).

References

Businger, J. A., Wyngaard, J. C., Izumi, Y., and Bradley, E. F.: 1971, 'Flux-profile relationships in the atmospheric surface layer' *J. Atmos. Sci.* 28, 181-189.

Charnock, H.: 1955, 'Wind stress over a water surface' *Quart. J. Roy. Meteor. Soc*. 81, 639-640.

Csanady, G. T.: 1974, 'Equilibrium theory of the planetary boundary layer with an inversion lid' *Boundary-Layer Meteorol.* 6, 63-79.

Edson, J. B., and Fairall, C. W.: 1998, 'Similarity relationships in the marine atmospheric surface layer for terms in the TKE and scalar variance budgets' *J. Atmos. Sci.* 55, 2311-2328.

Fairall, C. W., Bradley, E. F., Godfrey, J. S., Wick, G. A., Edson, J. B. and Young, G. S.: 1996, 'Cool-skin and warm-layer effects on sea surface temperature' *J. Geophys. Res.* 101(C1), 1295-1308.

Garratt, J. R.: 1987, 'The stably stratified internal boundary layer for steady and diurnally varying offshore flow', *Boundary-Layer Meteorol*. 38, 169-394.

Garratt, J. R., and Ryan B. F.: 1989, 'The structure of the stably stratified internal boundary layer in offshore flow over the sea' *Boundary-Layer Meteorol.* 47, 17-40.

Garratt, J. R.: 1994, *The atmospheric boundary layer*, Cambridge University Press, Cambridge, 316 pp.

Geernaert, G., and Larsen, S.: 1993, 'On the role of humidity in estimating marine surface layer stratification and scaterometer cross section' *J. Geophys. Res.* 98(C1), 927-932.

Grachev, A. A., and Fairall C. W.: 1997, 'Dependence of the Monin-Obukhov stability parameter on the bulk Richardson number over the Ocean' *J. Appl. Meteor.* 36, 406-414.

Högström, U.: 1988, 'Nondimensional wind and temperature profiles' *Boundary-Layer Meteorol.* 42, 55-78.

Højstrup, J.: 1999, 'Vertical Extrapolation of Offshore Wind Profiles' in E. L. Petersen, P. Hjuler Jensen, K. Rave, P. Helm, H. Ehmann (eds.), *Wind energy for the next millennium. Proceedings. 1999 European wind energy conference (EWEC '99)*,

Nice, FR, March 1—5, 1999, James and James Science Publishers, London, U.K., pp. 1220-1223.

Johnson, H. K., Højstrup, J., Vested H. J., and Larsen S. E.: 1998, 'On the Dependence of Sea Surface Roughness on Wind Waves' *J. Phys. Oceanogr.* 28, 1702-1716.

Källstrand, B.: 1998, 'Low level jets in a marine boundary layer during spring' *Contr. Atmos. Phys.* 71, 359-373.

Kristensen, L.: 1998, 'Cup anemometer behaviour in turbulent environments' *J. Atmos. Oceanic Tech*. 15, 5-17.

Lange, B., Barthelmie R. J., and Højstrup J.: 2001, *Description of the Rødsand field measurement,* Report Risø-R-1268, Risø National Laboratory, 4000 Roskilde, DK, 60 pp.

Larsen, S. E.: 1993, 'Observing and modelling the planetary boundary layer' in E. Raschke and D. Jacob (eds.), *Energy and water cycles in the climate system,* NATO ASI series I, volume 5, Springer-Verlag, Berlin, Heidelberg, pp. 365-418.

Lange, B., Johnson, H.K., Larsen, S., Højstrup, J., Kofoed-Hansen, H. and Yelland, M.J.: 2003, 'On detection of a wave age dependency for the sea surface roughness' manuscript accepted by *J. Phys. Oceanog.*

Lenschow D. H., Li X. S. , Zhu C. J., and Stankov, B. B.: 1988, 'The stably stratified boundary layer over the Great Plains, I, Mean and turbulence structure' *Boundary-Layer Meteorol.* 42, 95-121.

Melas, D.: 1989, 'The temperature structure in a stably stratified internal boundary layer over a cold sea' *Boundary-Layer Meteorol.* 48, 361-375.

Mortensen, N. G., Landberg L., Troen, I., and Petersen, E. L.: 1993, *Wind Analysis and Application Program (WASP) - User's Guide,* Report Risø-I-666(EN) (v.2), Risø National Laboratory, 4000 Roskilde, DK, 133 pp.

Panofsky, H. A.: 1973, 'Tower Micrometeorology', in D.A. Haugen (ed.), *Workshop on Micrometeorology*, American Meteorological Society, Boston, pp. 151-176.

Schotanus, P., Nieuwstadt, F.T.M. and De Bruin, H.A.R.: 1983, 'Temperature measurement with a sonic anemometer and its application to heat and moisture fluxes' *Boundary-Layer Meteorol.* 26, 81-93.

Smedman, A.-S., Bergström, H. and Grisogono, B.: 1997, 'Evolution of stable internal boundary layers over a cold sea' *J. Geophys. Res.* 102(C1), 1091-1099.

Tennekes, H.: 1982, 'Similarity relations, scaling laws and spectral dynamics', in F. T. M. Nieuwstadt, and H. van Dop (eds.), *Atmospheric turbulence and air pollution modelling*, Reidel, Hingham, MA, pp.37-68.

Tjernström, M., and Smedman, A.-S.: 1993, 'The vertical turbulence structure of the coastal marine atmospheric boundary layer', *J. Geophys. Res.* 98(C3), 4809-4826.

Wu, J.: 1980, 'Wind stress Coefficients over Sea Surface near Neutral Conditions – A Revisit', *J. Phys. Oceanogr*. 10, 727-740.

Wyngaard, J. C.: 1973, 'On surface-layer turbulence', in D.A. Haugen (ed.), *Workshop on Micrometeorology*, American Meteorological Society, Boston, pp. 101-149.

Figure captions

Figure 1: Map of measurement stations

Figure 2: Ratios of wind speed at 50 and 10 m height at Rødsand versus the stability parameter 10/L with L derived from the sonic anemometer measurements; data with fetch <20km are marked; also shown is the prediction of Monin-Obukhov theory

Figure 3: Ratios of wind speed at 50 and 10 m height at Rødsand versus the stability parameter 10/L with L derived from the wind and temperature difference measurements at 10 and 50 m height; data with fetch <20km are marked; also shown is the prediction of Monin-Obukhov theory

Figure 4: Ratios of wind speed at 50 and 10 m height at Rødsand versus the stability parameter 10/L with L derived from the bulk method (see text); data with fetch <20km are marked; also shown is the prediction of Monin-Obukhov theory

Figure 5: Bin-averaged ratio of measured and predicted 50 m wind speed versus stability parameter 10/L with L determined by the sonic, gradient and bulk methods

Figure 6: Bin-averaged ratio of measured and predicted 50 m wind speed versus stability parameter 10/L with L determined by the bulk method; three different methods to estimate the sea surface roughness have been used in the predictions: Constant sea surface roughness, Charnock relation and a wave age dependent extension of the Charnock relation

Figure 7: Time series of measurements at Rødsand for 15 and 16 January 1999; shown are air temperatures at 10m height and over upwind land (see section 2.4)

and water temperature (uppermost panel); wind speeds at 10 m height and wind directions at Rødsand and over land (second panel); ratio of measured and predicted wind speed at 50 m height with three methods to determine L (sonic, gradient and bulk)(third panel); stability parameter S and buoyancy parameter Bu (lowest panel)

Figure 8: As above, but for 24 January 1999

Figure 9: Scatter plot of ratio of measured and predicted (gradient method for L, Charnock equation for z_0) wind speed at 50 m height versus temperature difference between air temperature over the upwind land area and the water temperature at Rødsand

Figure 10: Scatter plot of ratio of measured and predicted (gradient method for L, Charnock equation for z_0) wind speed at 50 m height versus buoyancy parameter Bu

Figure 11: Ageosprophic angle α versus stability parameter μ=h/L for typical surface roughness of land (0.1m) and sea (0.0001m) for slightly stable conditions

Figure 12: Measured difference in surface wind direction measured at the upwind land station and Rødsand versus the buoyancy parameter Bu; also shown are the range expected from conventional theory for slightly stable boundary layers and an extrapolation to the limit of 60° difference at Bu=500 predicted by Csanady (1974)

Figure 13: Scatter plot of ratio of measured and predicted (gradient method for L, Charnock equation for z_0) wind speed at 50 m height versus bulk stability parameter S

Figure 14: Scatter plot of ratio of measured and predicted (gradient method for L, Charnock equation for z_0) wind speed at 50 m height versus mixed layer depth h after Csanady (1974)

Table captions

Table 1**:** Instrumentation of the Rødsand measurement

Table 2: Comparison of different methods to predict the wind speed at 50 m height from the 10m wind; Bias and standard deviation of modelled time series compared to the measured one are shown for all data and separately for stable and unstable conditions

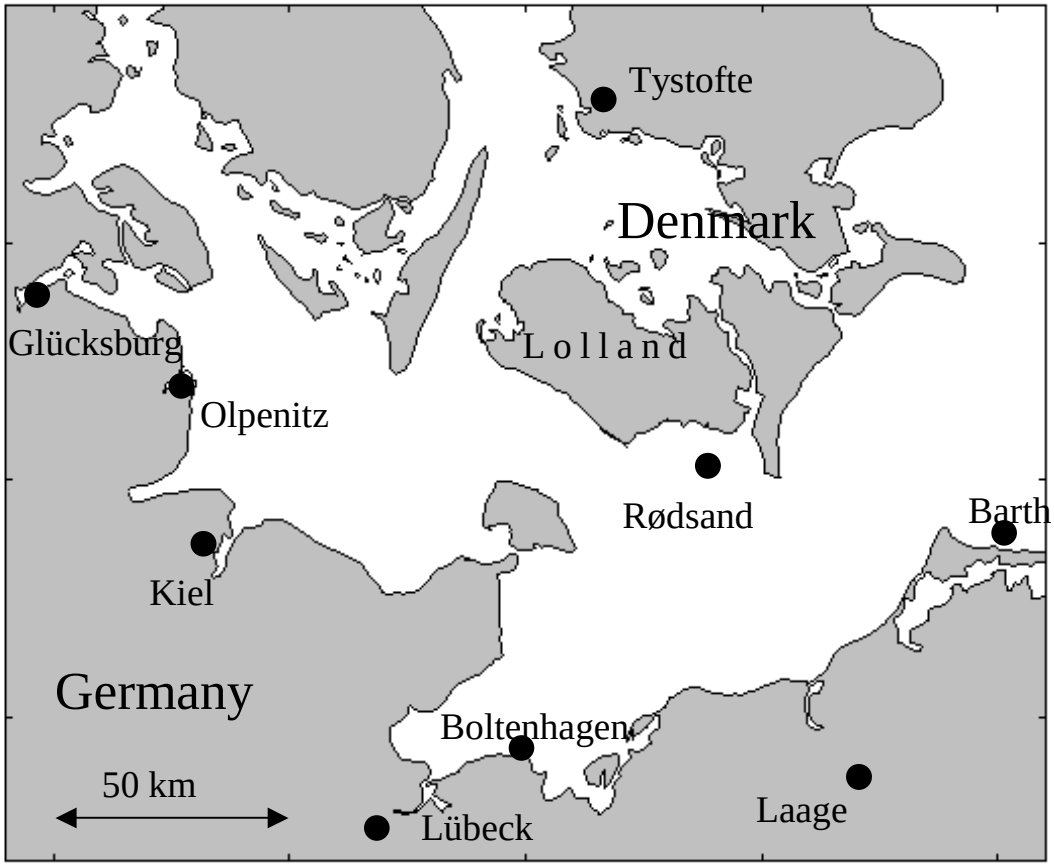

Figure 1: Map of measurement stations

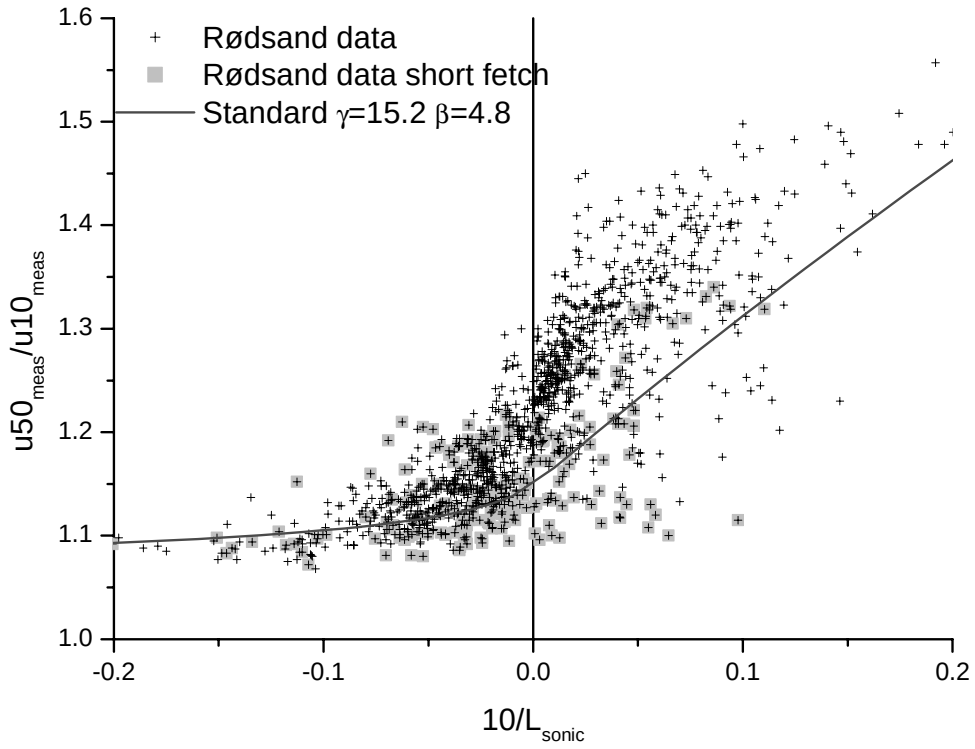

Figure 2: Ratios of wind speed at 50 and 10 m height at Rødsand versus the stability parameter 10/L with L derived from the sonic anemometer measurements; data with fetch <20 km are marked; also shown is the prediction of Monin-Obukhov theory

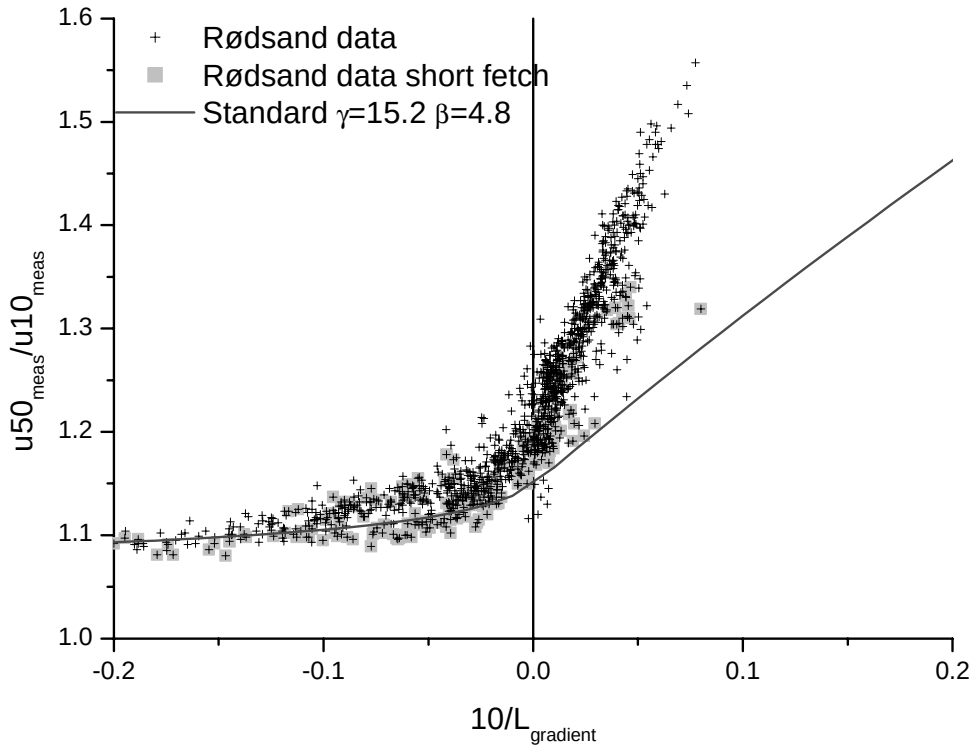

Figure 3: Ratios of wind speed at 50 and 10 m height at Rødsand versus the stability parameter 10/L with L derived from the wind and temperature difference measurements at 10 and 50 m height; data with fetch <20 km are marked; also shown is the prediction of Monin-Obukhov theory

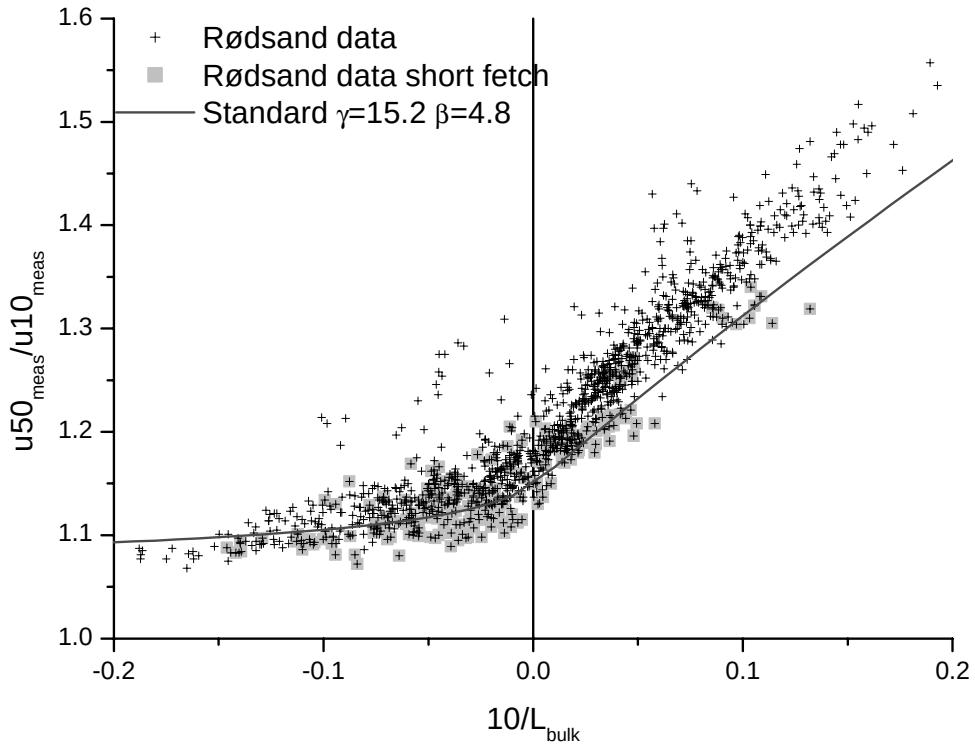

Figure 4: Ratios of wind speed at 50 and 10 m height at Rødsand versus the stability parameter 10/L with L derived from the bulk method (see text); data with fetch <20 km are marked; also shown is the prediction of Monin-Obukhov theory

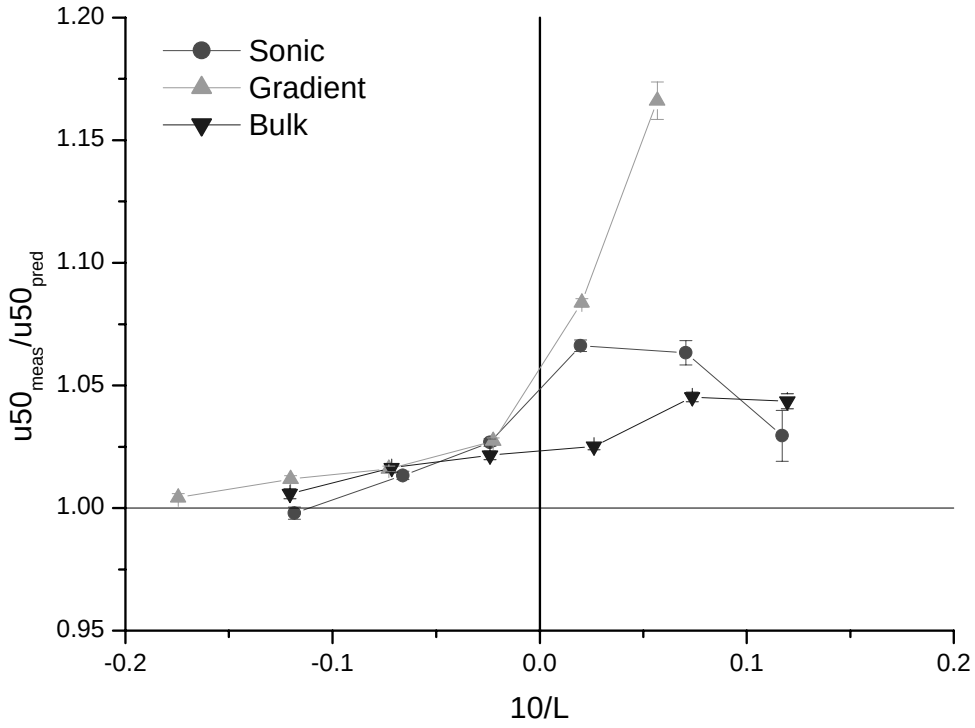

Figure 5: Bin-averaged ratio of measured and predicted 50 m wind speed versus stability parameter 10/L with L determined by the sonic, gradient and bulk methods

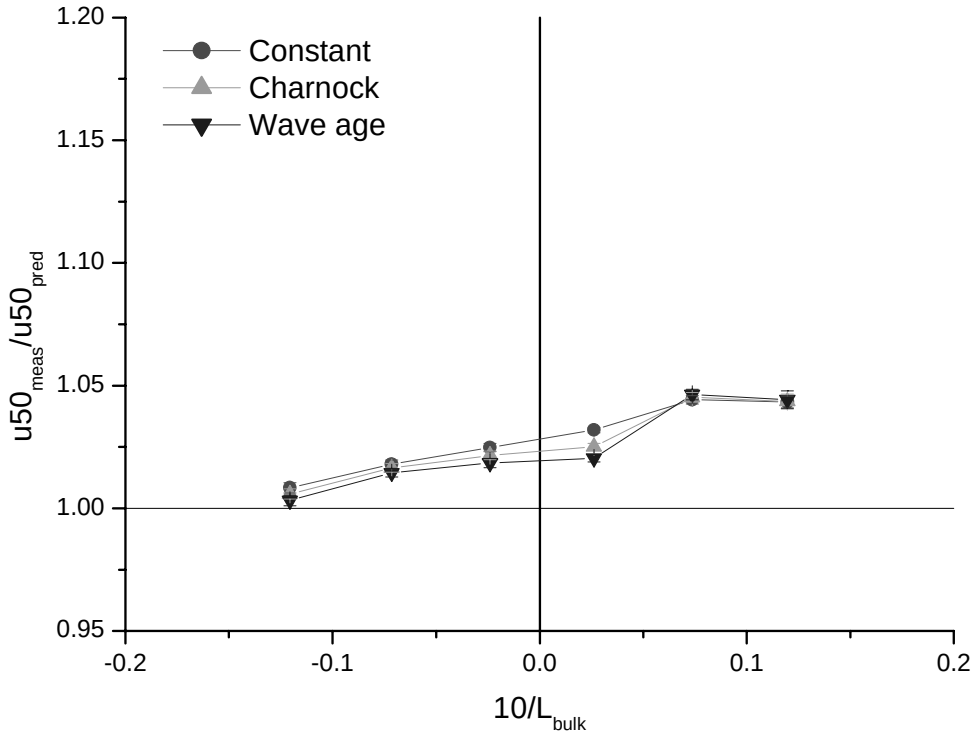

Figure 6: Bin-averaged ratio of measured and predicted 50 m wind speed versus stability parameter 10/L with L determined by the bulk method; three different methods to estimate the sea surface roughness have been used in the predictions: Constant sea surface roughness, Charnock relation and a wave age dependent extension of the Charnock relation

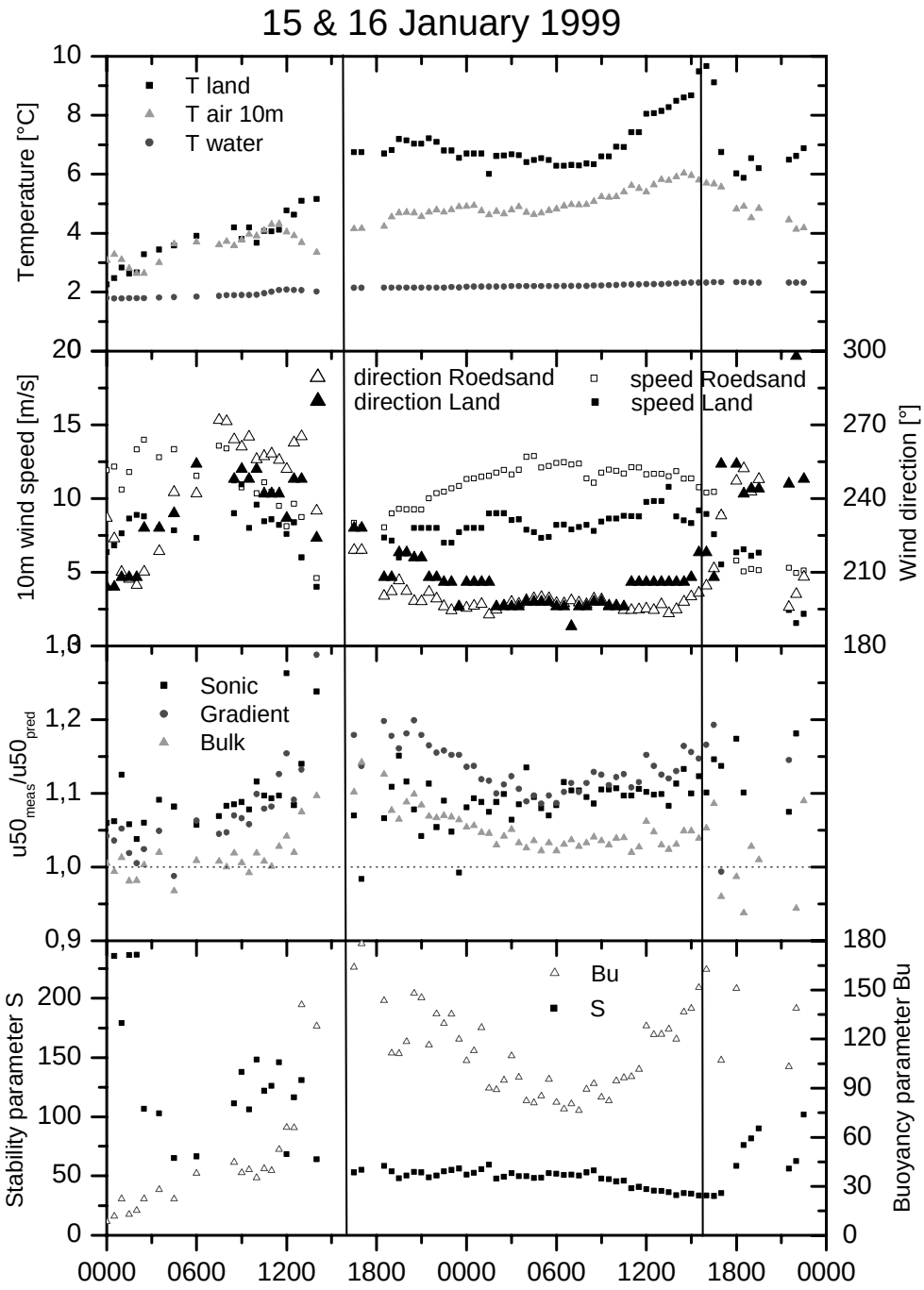
15 & 16 January 1999
Temperature [°C]
T land
T air 10m
T water
10m wind speed [m/s]
Wind direction [°]
direction Roedsand
direction Land
speed Roedsand
speed Land
u50meas/u50pred
Sonic
Gradient
Bulk
Stability parameter S
Buoyancy parameter Bu
Bu
S
0000
0600
1200
1800
0000
0600
1200
1800
0000

Figure 7: Time series of measurements at Rødsand for 15 and 16 January 1999; shown are air temperatures at 10m height and over upwind land (see section 2.4) and water temperature (uppermost panel); wind speeds at 10 m height and wind directions at Rødsand and over land (second panel); ratio of measured and predicted wind speed at 50 m height with three methods to determine L (sonic, gradient and bulk)(third panel); stability parameter S and buoyancy parameter Bu (lowest panel)

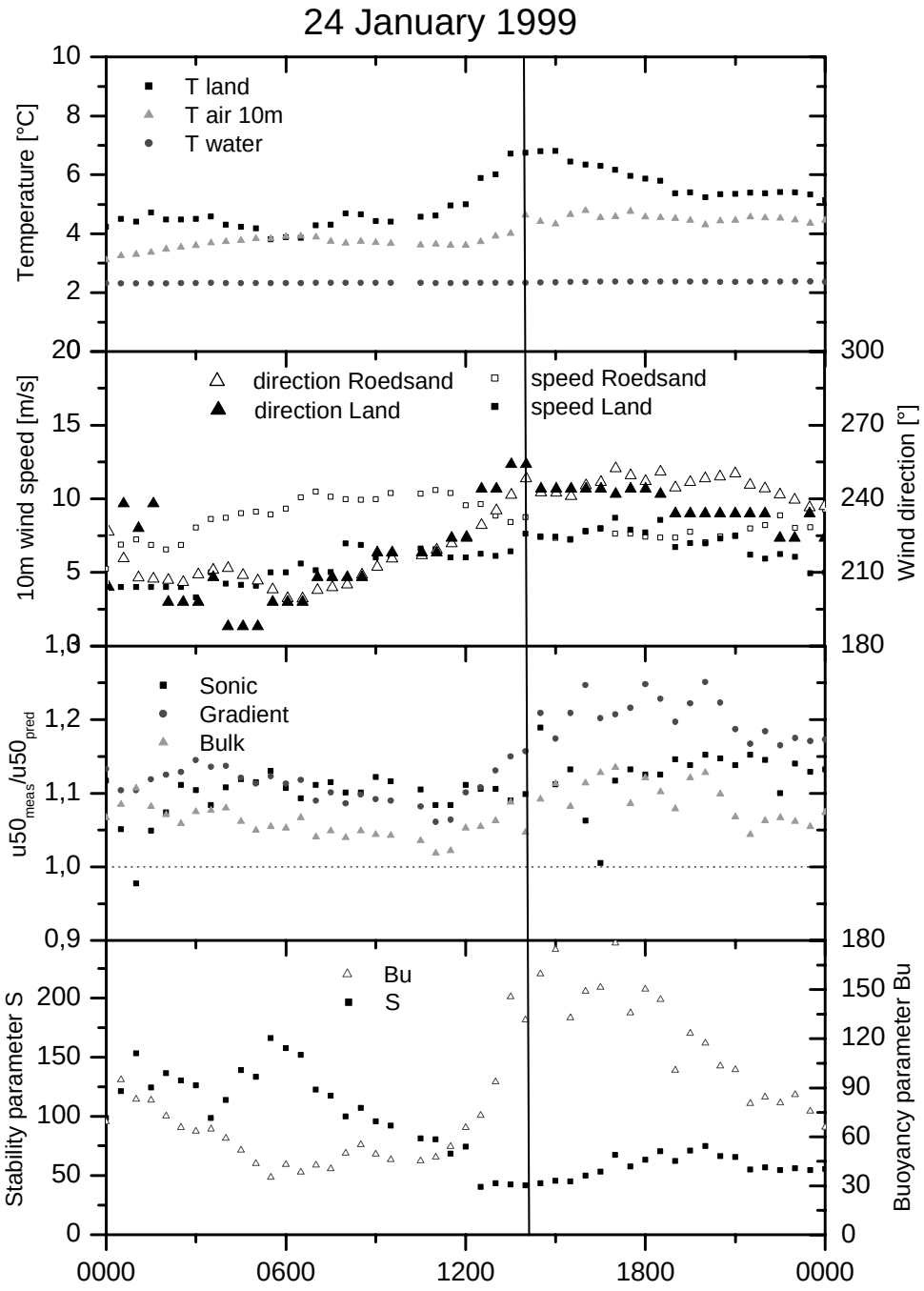

Figure 8: As above, but for 24 January 1999

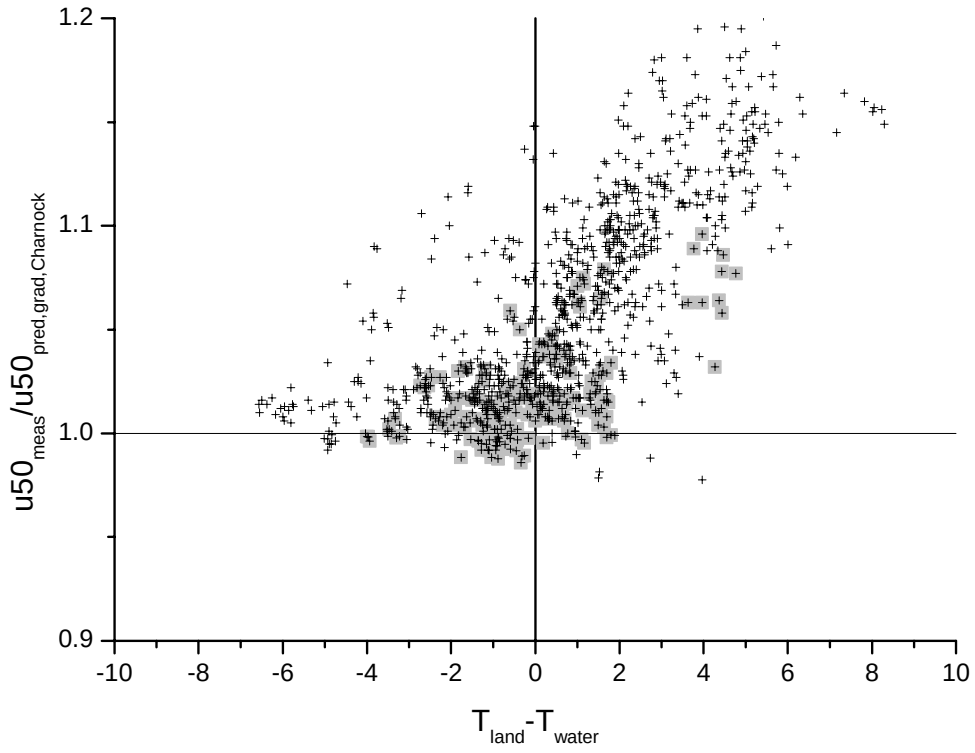

Figure 9: Scatter plot of ratio of measured and predicted (gradient method for L, Charnock equation for z_0) wind speed at 50 m height versus temperature difference between air temperature over the upwind land area and the water temperature at Rødsand

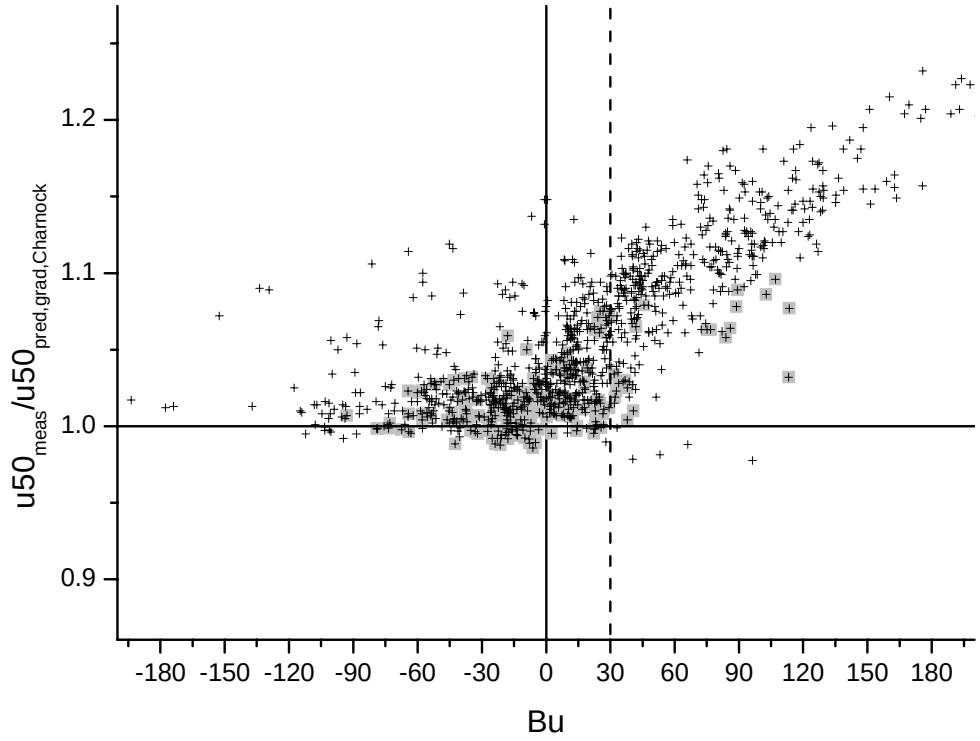

Figure 10: Scatter plot of ratio of measured and predicted (gradient method for L, Charnock equation for z_0) wind speed at 50 m height versus buoyancy parameter Bu

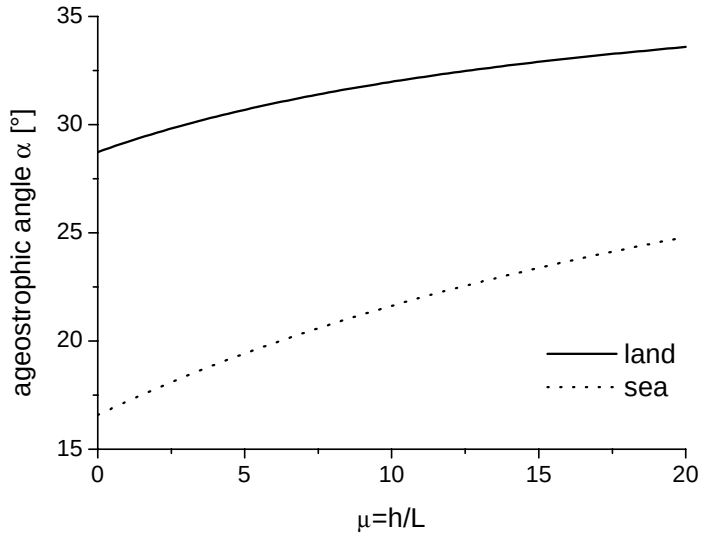

Figure 11: Ageostrophic angle α versus stability parameter μ=h/L for typical surface roughness of land (0.1m) and sea (0.0001m) for slightly stable conditions

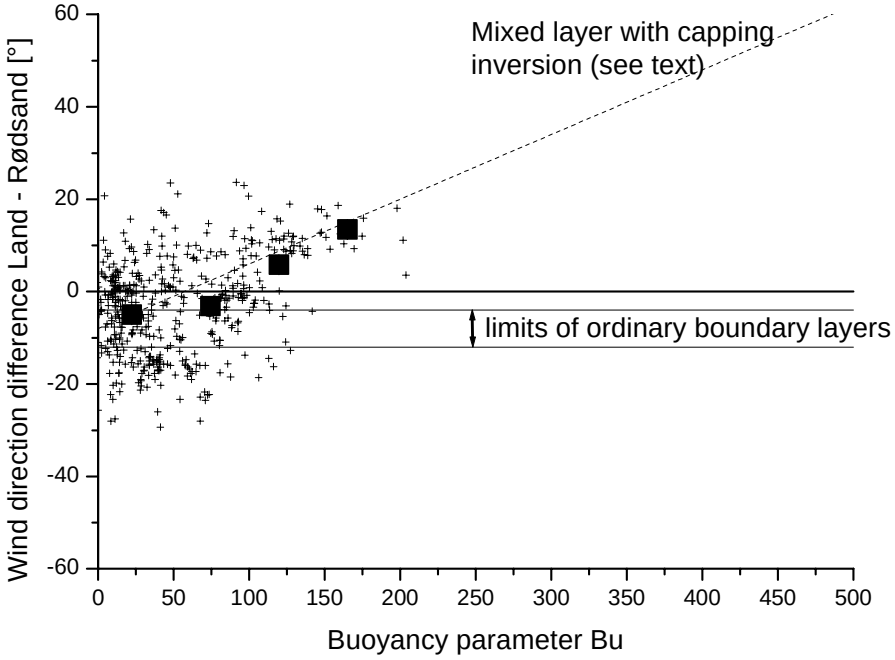

Figure 12: Measured difference in surface wind direction of the upwind land station and Rødsand versus the buoyancy parameter Bu: data (crosses) and bin averages (squares); also shown are the range expected from conventional theory for slightly stable boundary layers and an extrapolation to the limit of 60° difference at Bu=500 predicted by Csanady (1974)

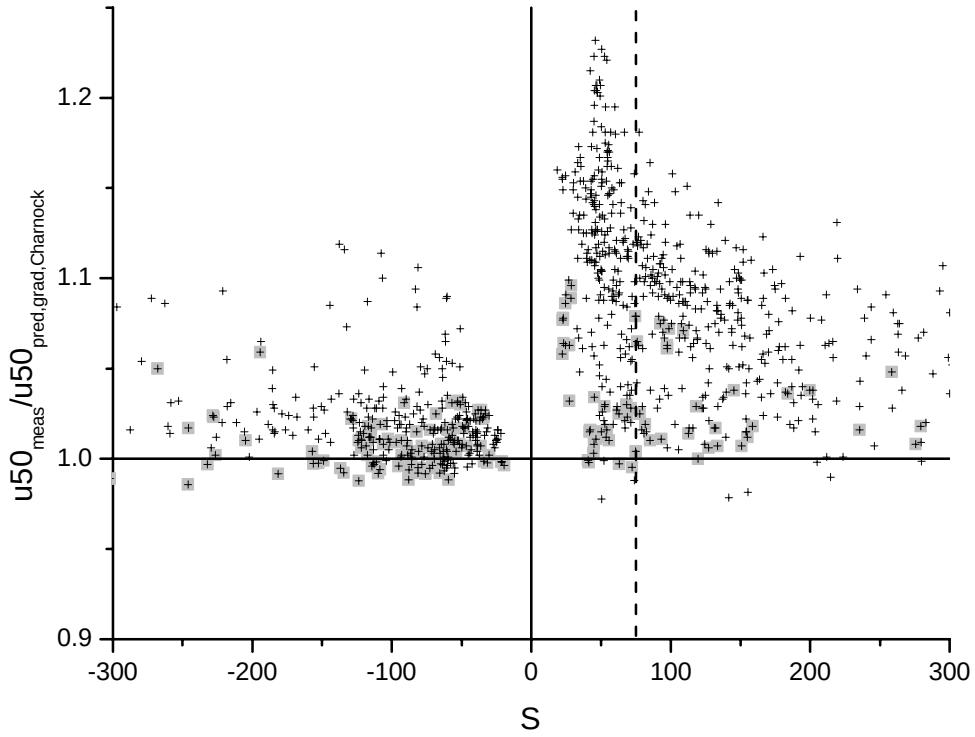

Figure 13: Scatter plot of ratio of measured and predicted (gradient method for L, Charnock equation for z_0) wind speed at 50 m height versus bulk stability parameter S

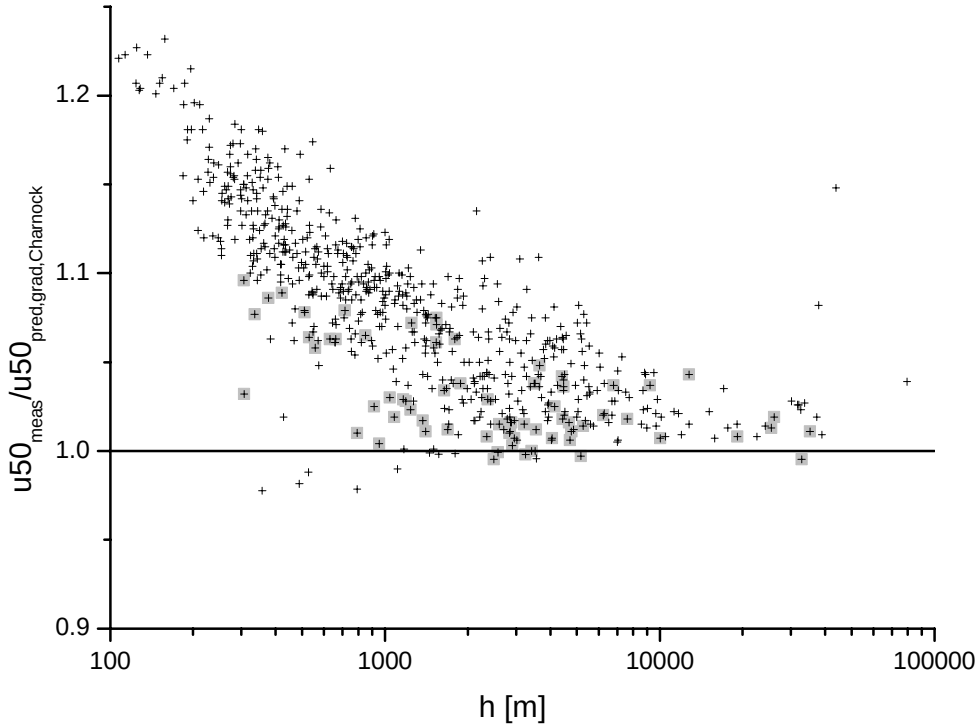

Figure 14: Scatter plot of ratio of measured and predicted (gradient method for L, Charnock equation for z_0) wind speed at 50 m height versus mixed layer depth h after Csanady (1974)

Table 1: Instrumentation of the Rødsand measurement

	height above mean sea level	instrument	sampling rate
Wind speed	50.3 m	cup anemometer	5 Hz
	29.8 m	cup anemometer	5 Hz
	10.2 m	cup anemometer	5 Hz
Wind direction	29.7 m	wind vane	5 Hz
3 axis wind speed and temperature	46.6 m (42.3 m from 12.5.99)	ultrasonic anemometer	20 Hz
Air temperature	10.0 m	Pt 100	30 min mean
Temperature difference	49.8 m – 10.0 m	Pt 500	30 min mean
Sea temperature	about –2m	Pt 100	30 min mean
Sea level		DHI AWR201 acoustic wave recorder	8 Hz
Sea current		GMI current meter	8 Hz

Table 2: Comparison of different methods to predict the wind speed at 50 m height from the 10m wind; Bias and standard deviation of modelled time series compared to the measured one are shown for all data and separately for stable and unstable conditions

	all data		stable data		unstable d.	
	bias [%]	rms [%]	bias [%]	rms [%]	bias [%]	rms [%]
L from Sonic method						
Constant	4.6	4.8	6.4	5.4	2.5	2.9
Charnock	4.3	4.9	6.3	5.4	2.1	2.9
Wave age	4.1	5.0	6.2	5.6	1.8	3.0
L from Gradient method						
Constant	5.9	4.8	9.1	4.3	2.4	2.0
Charnock	5.7	5.0	9.0	4.7	2.0	2.0
Wave age	5.5	5.3	8.9	5.0	1.7	2.1
L from Bulk method						
Constant	3.0	2.7	4.2	2.8	1.7	1.8
Charnock	2.7	3.0	4.0	3.2	1.3	1.8
Wave age	2.5	3.3	3.9	3.7	0.9	2.0